GENERAL ATOMIC
DIVISION OF GENERAL DYNAMICS

GA-4258

HIGH-TEMPERATURE VAPOR-FILLED THERMIONIC CONVERTER

QUARTERLY TECHNICAL PROGRESS REPORT
FOR THE PERIOD
ENDING APRIL 30, 1963

Contract AF 33(657)-8563
Project No. 8173, Task No. 817305-5

Aeronautical Systems Division
Air Force Systems Command
U. S. Air Force
Wright-Patterson Air Force Base, Ohio

May 17, 1963

GENERAL ATOMIC

DIVISION OF

GENERAL DYNAMICS

JOHN JAY HOPKINS LABORATORY FOR PURE AND APPLIED SCIENCE

P.O. BOX 608, SAN DIEGO 12, CALIFORNIA

GA-4258

HIGH-TEMPERATURE VAPOR-FILLED THERMIONIC CONVERTER

QUARTERLY TECHNICAL PROGRESS REPORT

FOR THE PERIOD

ENDING APRIL 30, 1963

Contract AF 33(657)-8563
Project No. 8173, Task No. 817305-5

Aeronautical Systems Division
Air Force Systems Command
U. S. Air Force
Wright-Patterson Air Force Base, Ohio

Work done by:

E. Gillette
W. Godsin
G. Hoover
R. Skoff
R. Schmeling
A. Weinberg
L. R. Zumwalt

Report written by:

W. Godsin
R. Skoff

May 17, 1963

FOREWARD

The work covered by this report was accomplished under Air Force Contract AF 33(657)-8563, but this report is being published and distributed prior to Air Force review. The publication of this report, therefore, does not constitute approval by the Air Force of the findings or conclusions contained herein. It is published for the exchange and stimulation of ideas.

INTRODUCTION

This report covers the quarterly period ending April 30, 1963, in accordance with Modification No. 1 to this contract. Also included, however, are the research results for the month of January, 1963.

TABLE OF CONTENTS

	Page
SUMMARY	1
GENERAL	3
CELL F	3
CELLS G, H, AND J	8
a. Cell Assembly	8
b. Cell Performance	10
OPERATION OF CELLS IN PARALLEL AND SERIES	26
FISSION-PRODUCT CONTAMINATION OF THERMIONIC CONVERTERS	31
REFERENCES	34

SUMMARY

Filament failure and power degradation forced discontinuation of the testing of Cell F. Post-operativc analysis revealed that the remaining emitter thermocouple had maintained its calibration and that vacuum emission currents were at least equal to the pre-lifetest values at high emitter temperature but exceeded the pre-lifetest values at lower emitter temperatures. A large leak was found in the emitter cavity, which explained the loss of cesium and the resulting power degradation as well as the erosion of the filament and filament holder. Chemical analysis of the emitter showed a loss of about 75% of the uranium. A structure rich in tantalum carbide had formed at the tantalum carbide interface and had penetrated the entire tantalum substrate.

Cells G and J were placed in operation, while Cell H was held as a standby.

The vacuum emission currents measured on the three cells showed reasonably good consistency, although the values of Cell G were higher by a factor of three over those of Cell H. At 2200°K a current of 3.3 amp/cm^2 was measured in Cell G.

The power output curves for both Cells G and J showed a peak at a cesium temperature of 600 to 620°K, with a sharp power reduction above 620°K. At constant cesium pressure the power output appears to be an exponential function of emitter temperature. A maximum power of 6.8 w/cm^2 was observed at an emitter temperature of 2120°K. The temperature effect of the collector was investigated between 840°K and 1030°K and found to be almost negligible in this range.

A maximum short-circuit current of 170 amp was observed in Cell G. The short-circuit current increased with increasing cesium pressure to

620°K and then decreased slightly, whereas the open-circuit voltage and the voltage of maximum power decreased linearly with increasing cesium temperature. For optimum cesium pressure the voltage at maximum power was 0.7 volt at 2000°K. The open-circuit voltage increased with increasing emitter temperature. The effective emissivity at 2000°K was found to be 0.55 and decreased with increasing emitter and collector temperature.

Cell G has operated for 1662 hr at a power level of 12 to 18 watts and 91 hr at 20 watts output. Cell J was operated at a power level of 12 to 17 watts for 1249 hr, at 30 watts for 24 hr, and at 40 watts for 151 hr. With the exception of filament failures, the operation was uninterrupted by primary or auxiliary component failures.

On two occasions the output of Cell G was electrically connected to that of Cell F or J, and operation in parallel and series was conducted. The data observed are in agreement with Ohm's law for direct current.

A theoretical study of cell contamination by fission products revealed that the fate of any one of the many elements may differ widely from that of others. The noble gases krypton and xenon presumably will have the least detrimental effect in a vented system. The electronegative fission products tend to combine with the cesium to some extent. Since the cesium reservoir will be at the lowest temperature in the cell, most of the condensates of the fission products should collect there. The remaining fission products will condense on the various components of the cell.

GENERAL

CELL F

The operation of Cell F for 484 hr and its performance characteristics were reported in Ref. 1. Because frequent filament failures were encountered, cell operation was intermittent. Near the termination of the test, the power output had decreased by an order of magnitude. Cell performance could, however, be improved by a factor of two by increasing the cesium reservoir temperature to 750°K (a very abnormal condition). The cell was dismantled after an operational period in which measurements of parallel and series operation with Cell G were conducted.

A check revealed a large leak in the emitter cavity, with smaller leaks in the electron-beam weld joining the large insulator to the copper base. The large leak explained the short filament life and erosion of the filament holder reported in Ref. 1. The loss of cesium undoubtedly was the major factor in the observed performance degradation.

With the collector removed, it could be seen that thermocouple No. 1, which had given low readings during the test, had pulled out of its cavity during operation. A vacuum emission run and recalibration of thermocouple No. 2 were conducted with a test collector. From Fig. 1 it can be seen that the original calibration agreed very well with that determined post-operatively, thus the temperature data from thermocouple No. 2 were considered reliable throughout the test.

A comparison of the saturated vacuum emission values obtained before and after cell operation showed good agreement at 2000°K. With decreasing temperature, the post-operational vacuum emission values were increasingly higher, and at 1600°K were higher by a factor of four than pre-operational data (Fig. 2). This is a strong indication that loss of cesium rather than emitter deterioration was responsible for the cell degradation.

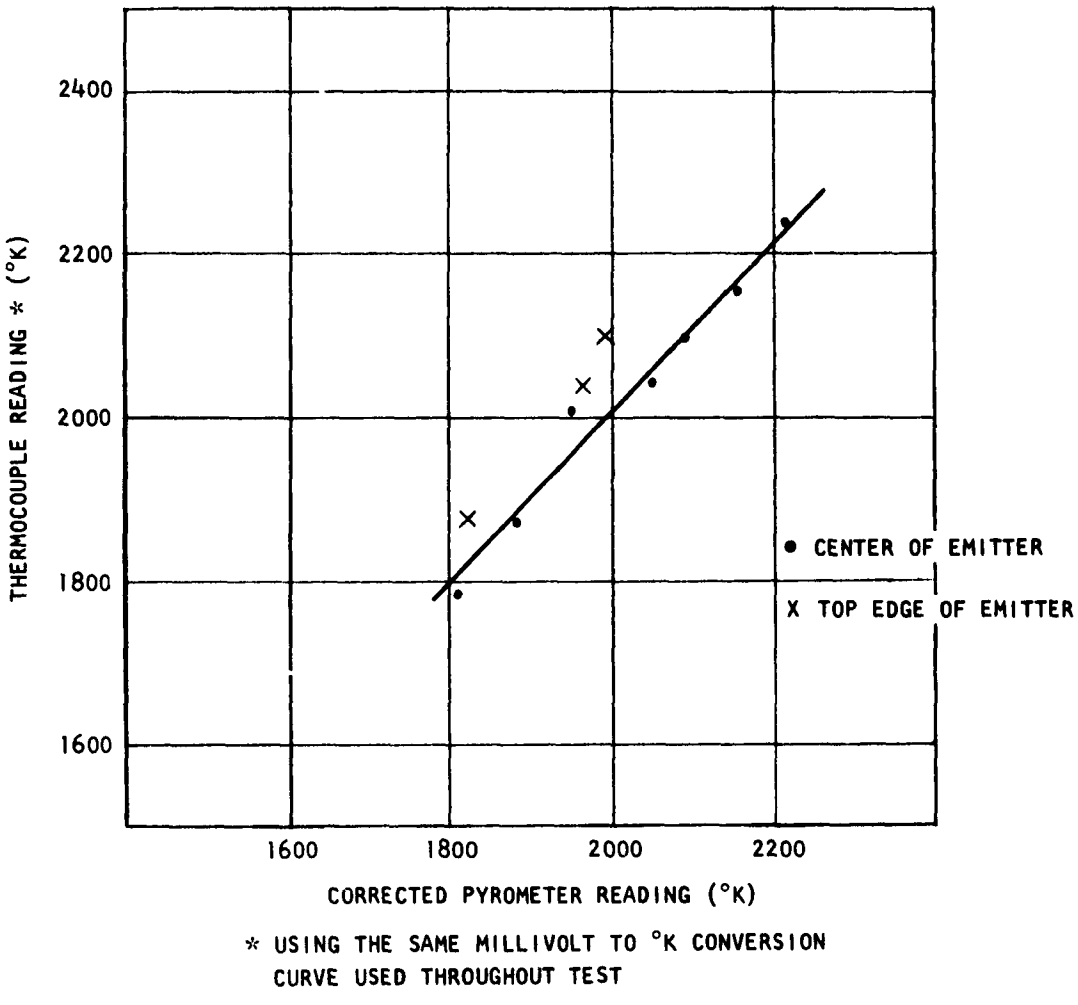

Fig. 1--Comparison of thermocouple and pyrometer reading of Cell F emitter temperature

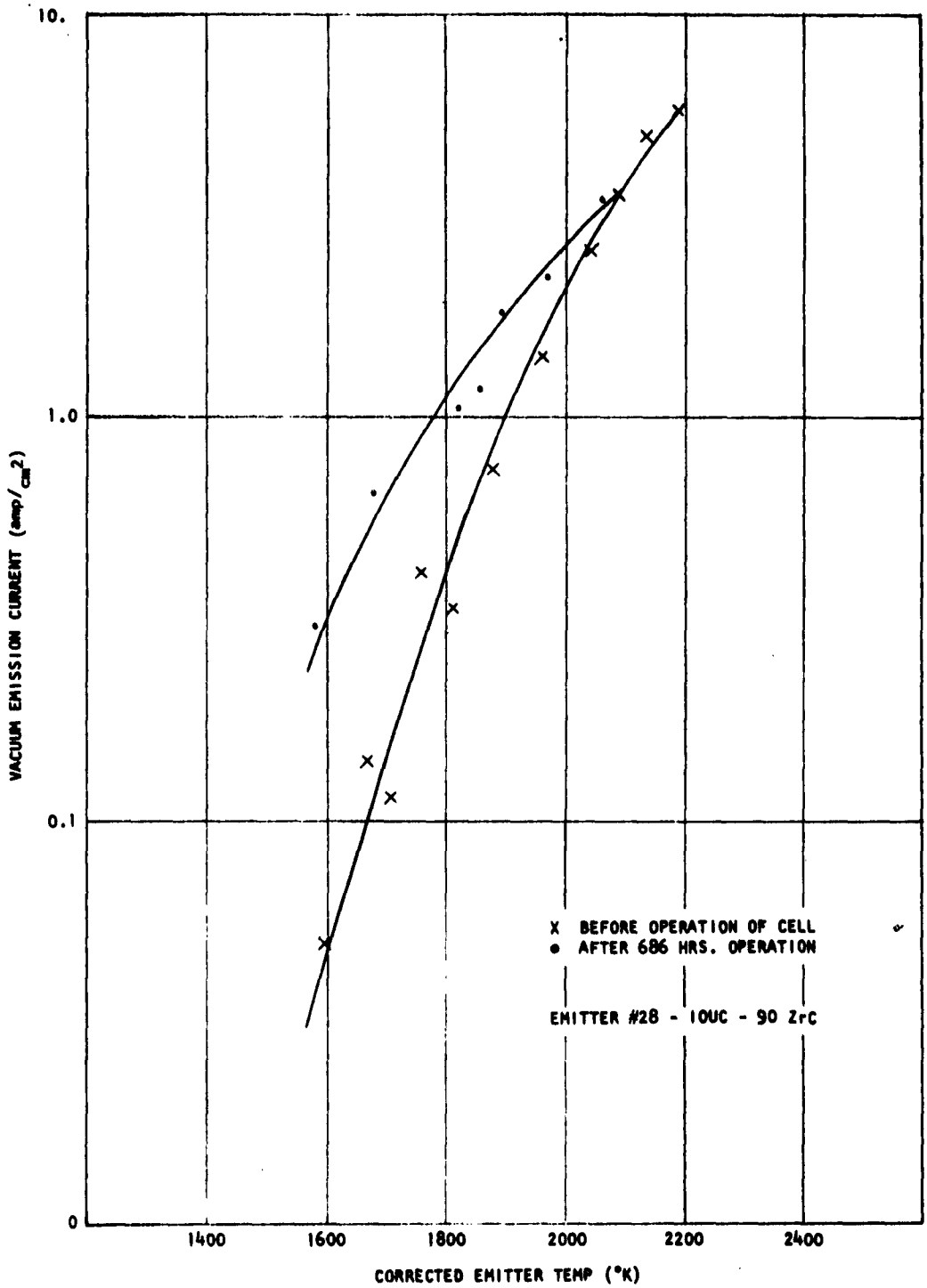

Fig. 2--Vacuum emission of Cell F at 3.5 kv

X-ray diffraction studies were made of the top of the emitter. The strongest was that of tungsten, while the ZrC pattern was weaker. Although the original powder contained some tungsten, it is believed that the tungsten from the filament of the electron gun deposited on the tantalum and then diffused through the large cracks observed in the emitter. The lack of a pattern corresponding to UC-ZrC indicates severe depletion of UC at the emitter surface.

The emitter was sectioned longitudinally for metallographic examination. The macrostructure of the emitter is illustrated in Fig. 3a. The cracks mentioned above are clearly visible. The emitter cavity had a tungsten coating. A brittle tantalum carbide structure was observed near the tantalum - UC-ZrC interface, which in some areas extended through the entire tantalum substrate (Fig. 3b). This reaction made free uranium available which migrated to the surface and then evaporated.

The results of the chemical analysis of the top and side of the emitter are tabulated below, together with the composition of the original powder used to make the emitter.

Emitter Material	Concentration (wt-%)				
	C	U	Zr	W	Ta
Original powder	10.20	19.67	67.02	4.16	--
Top - after lifetest	8.16	13.6	72.5	1.7	3.8
Side - after lifetest	7.86	5.32	80.63	1.2	2.5

The decrease in carbon content is in agreement with the metallographic observation of tantalum carbide formation. The cylindrical surface, which had been hotter, showed a greater decrease in uranium than the top.

The condensate in the collector cavity was black, hard, and crusty. A portion could be removed by scraping, while the remainder was leached

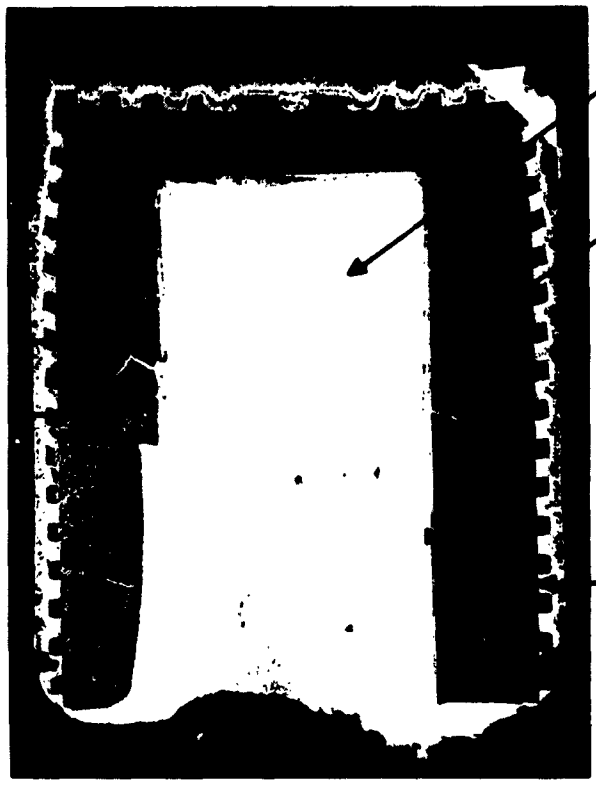

(a) Over-all section

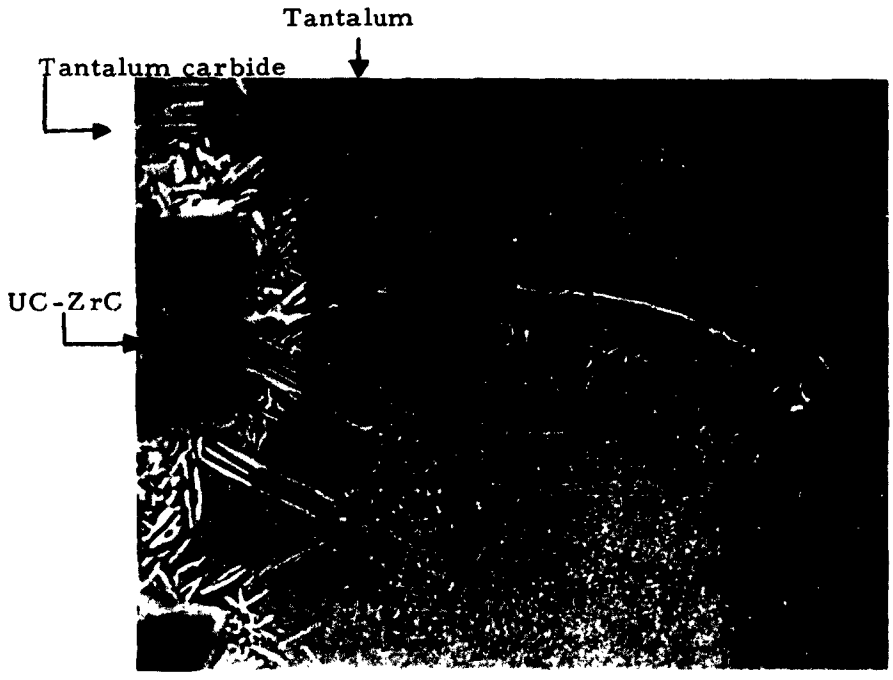

(b) Enlarged view; note carbide formation and crack propagation

Fig. 3--Longitudinal section of Mark V-F emitter

out with acid. These two fractions had different U/Zr ratios, indicating that they were of a different nature. The chemical analysis of the two portions is listed below:

Amount Collected	Concentration (wt-%)		
	U	Zr	C
0.1825 g by scraping	41.2	55.9	2.9
0.5710 g by leaching	90.2	9.8	Not determined
Total residue 0.7535 g			

While the scrapings contained 40 wt-% nickel from the collector, the nickel content was not determined in the leached solution since it was a function of leaching time only. A qualitative spectroscopic analysis revealed no other elements. The analysis of the emitter and collector is in good agreement with that of Cell E (Ref. 2). The major difference between the analyses of Cell E and Cell F was that no oxide pattern was found in the latter; otherwise, one analysis substantiated the other.

CELLS G, H, AND J

a. Cell Assembly

Cell G was prepared for operation after the assembly difficulties previously reported (Ref. 1) were overcome. Fig. 4 shows the cell in the vacuum stand ready for operation.

A vacuum emission test of Cell H, however, indicated contamination of the emitter surface. When the collector was removed, it was apparent that the cell had inadvertently been exposed to air while hot. The emitter stem had embrittled completely. A new emitter was subsequently welded in place and the cell assembly completed to the point of, but not including, breaking the cesium vial. Cell H was held as a standby.

Assembly of Cell J was completed and it was also placed in operation in this reporting period.

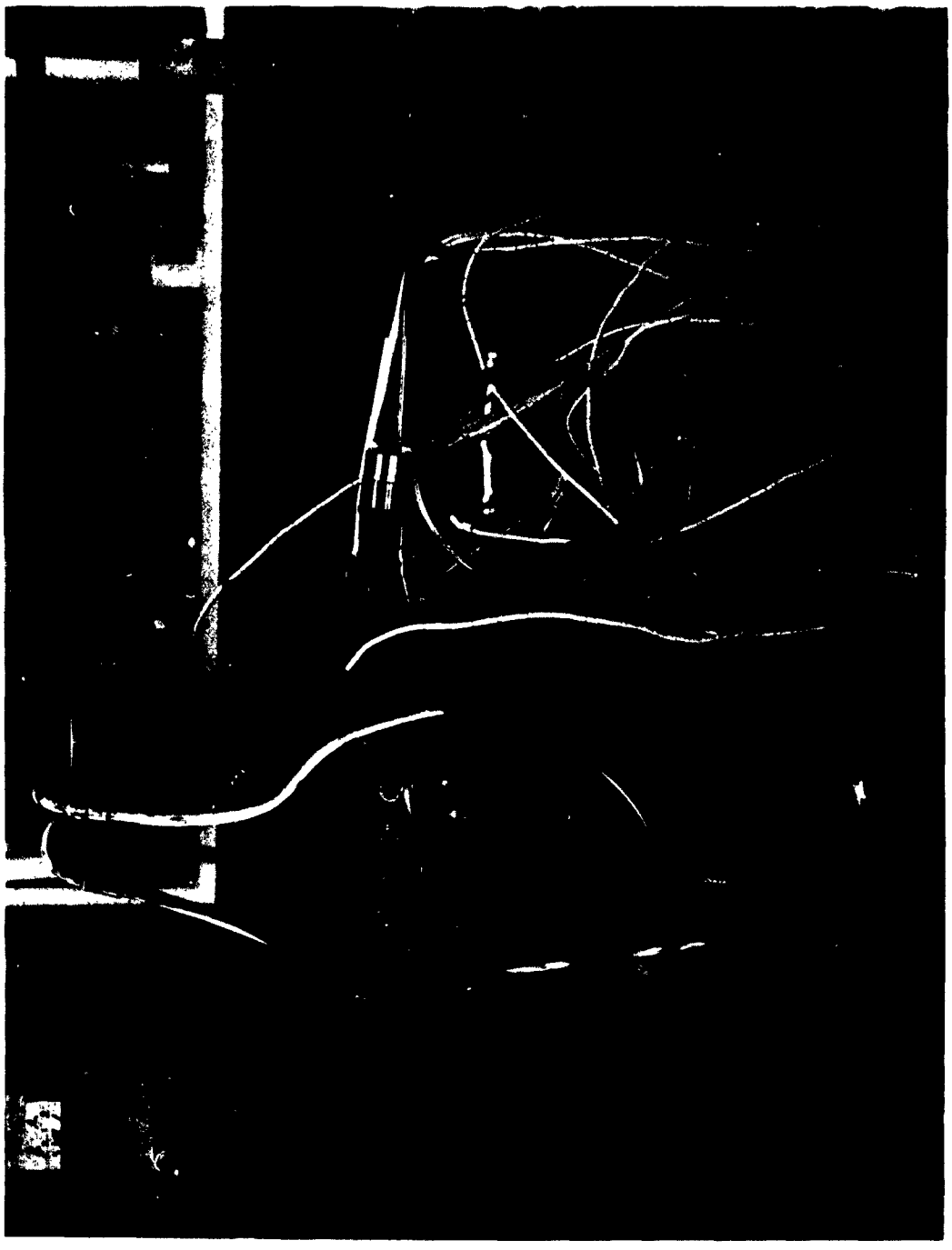

Fig. 4--Cell G in vacuum stand

b. Cell Performance

Vacuum emission studies were conducted on all cells with a test collector. Concurrently, the two emitter thermocouples were calibrated against surface temperature measurements made with an optical pyrometer. After welding the actual collector onto the cell, another vacuum emission test was conducted as a check on the final closure of the cell. Fig. 5 is a comparison of the saturated vacuum emission currents for the three cells before and after the final closure of the cell. The data spread for the various emitters is believed to be primarily due to different temperature distributions over the emitter surfaces, resulting in a different average surface temperature and current density. The thermocouples were calibrated against a pyrometer measurement taken at the hottest of the two sight holes in the test collector. Variations in surface condition have also contributed to differences in vacuum emission data.

After the introduction of cesium into the cells, the effect of cesium pressure on cell performance was studied with both Cells G and J. Fig. 6 is a plot of power output as a function of cesium pressure at an emitter temperature of 2000°K. Power output gradually increased as the cesium well temperature increased from 520°K to 600°K. A sharp decrease was observed at temperatures in excess of 620°K. Between 600 and 620°K the curve is fairly flat. The cesium temperature of Cells J and G was maintained predominantly between 603 and 610°K and 608 and 620°K, respectively.

The emitter temperature was varied between 1800 and 2200°K and the effect on power output, short-circuit current, and open-circuit voltage was investigated at constant cesium pressure.

The power output was determined to be an exponential function of the emitter temperature (Fig. 7), making it very sensitive to emitter temperature variations. At high temperatures, the power output of Cell G was twice that of Cell J. At an emitter temperature of 2110°K, a maximum power output of 68 watts from Cell G was observed; this is equivalent to

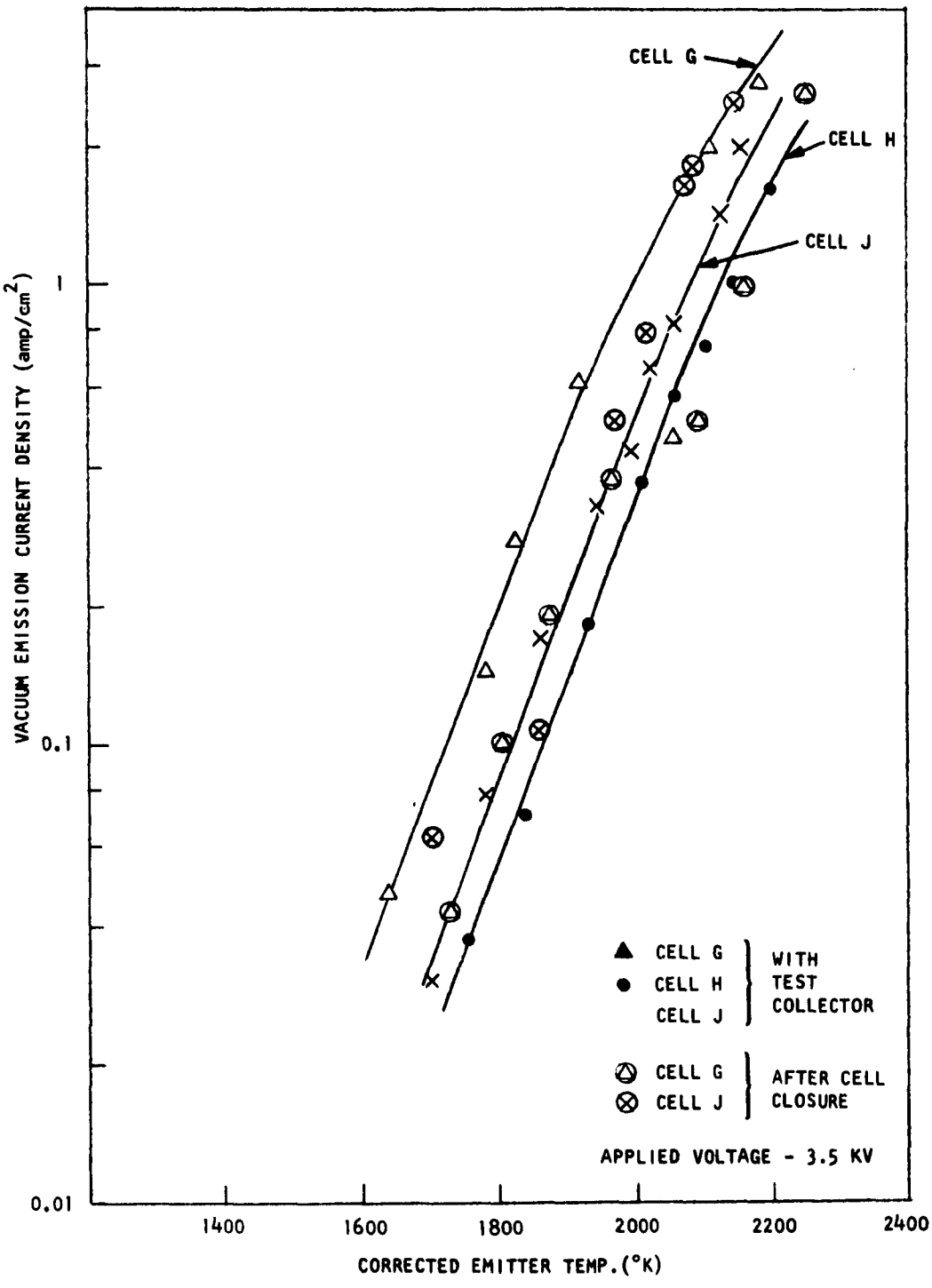

Fig. 5--Saturated vacuum emission of three cells before and after final cell closure

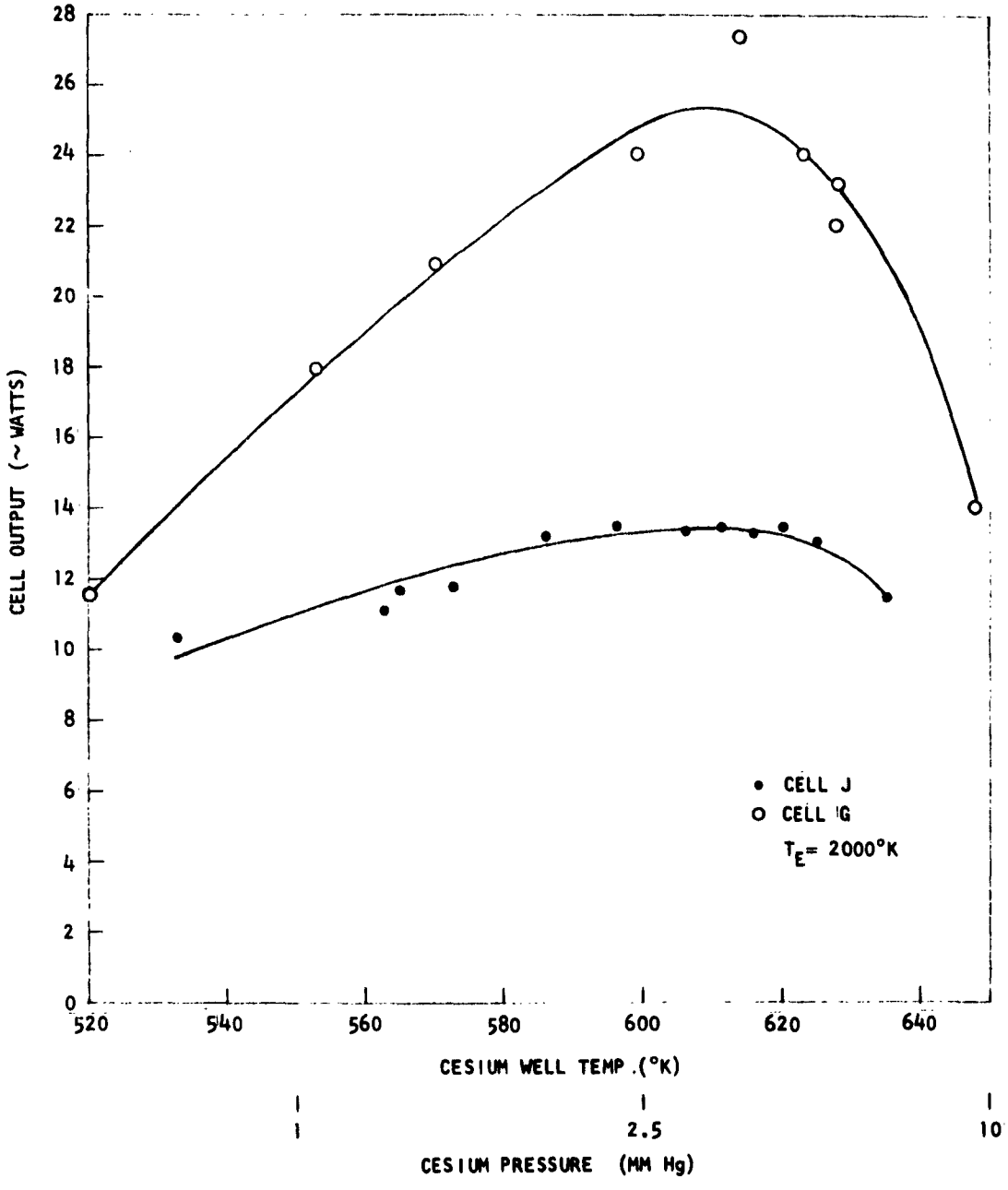

Fig. 6--Variation of power output of Cells G and J with cesium temperature and pressure

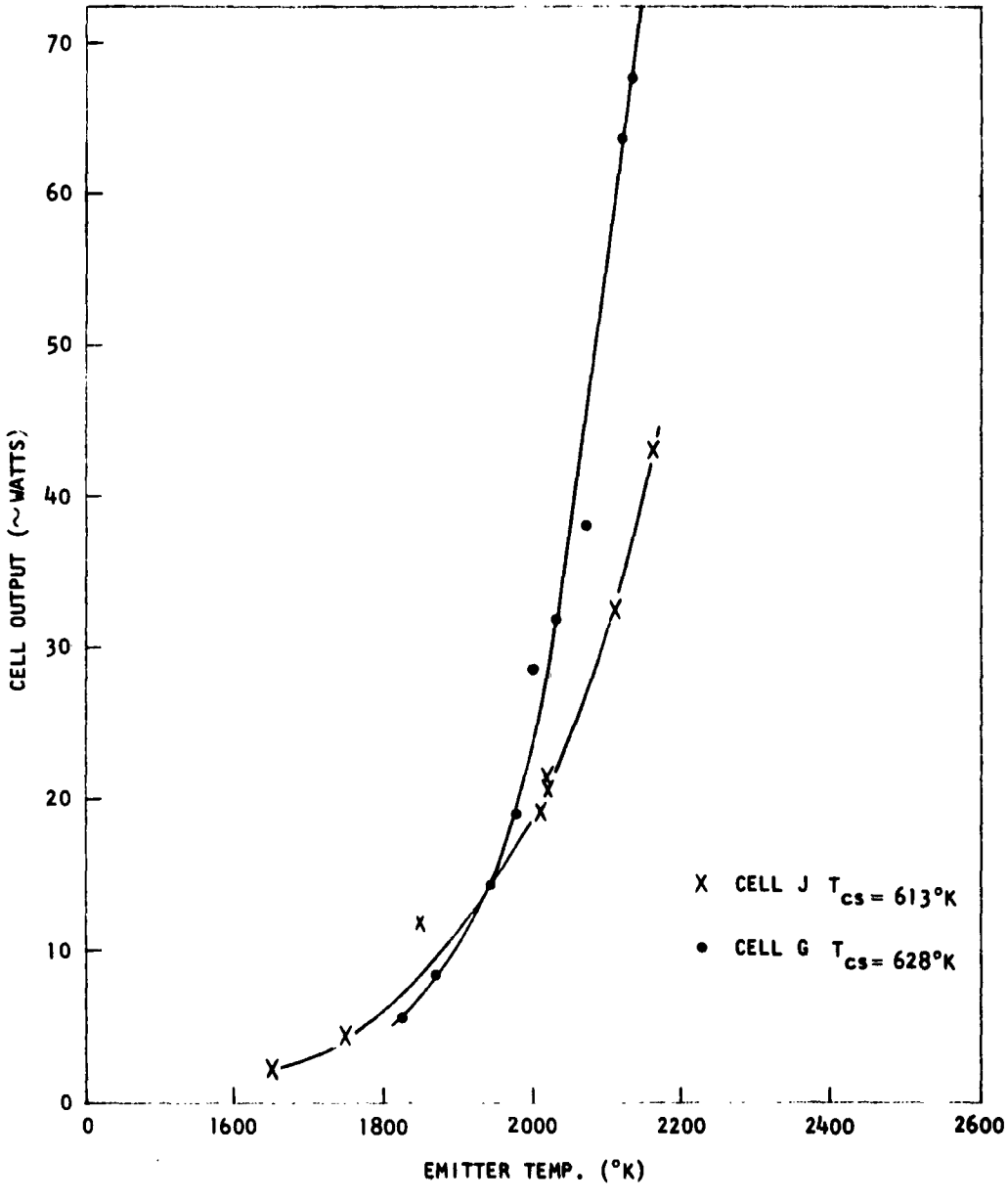

Fig. 7--Power output of Cells G and J as a function of emitter temperature

6.8 w/cm^2 for an emitting area of 10 cm^2. The total emitter surface area is 12 cm^2, but it appears that the area of the top (2 cm^2) does not contribute significantly to current emission because of its lower operating temperature and its much larger spacing (~ 100 mils).

The effect of collector temperatures on power output was determined between the temperatures 840°K and 1030°K. The collector temperature was controlled by varying the coolant flow and by adding auxiliary heat from an electrical heater on the collector. From Fig. 8 it can be seen that the collector temperature, in the ranges investigated, had no significant effect on the power output. During the latter part of the operational life of both cells, the coolant flow was stopped completely and the collector temperatures drifted to as high as 1250°K due to higher emitter temperatures. There was no apparent evidence of a large degradation of power attributable to this high collector temperature. In contrast, Cell F (Ref. 1) exhibited a 20% power loss for an increase in collector temperature of 100°C.

The short-circuit current density is shown as a function of emitter temperature in Figs. 9 and 10 for Cells G and J, respectively. The short-circuit current was determined from oscilloscope pictures at the point where the cell voltage was zero. The maximum short-circuit current observed in Cell G was 170 amp at an emitter temperature of 2120°K, a collector temperature of 953°K, and a cesium temperature of 628°K. The maximum short-circuit current recorded for Cell J was 110 amp at 2200°K emitter temperature (cesium temperature = 606°K). The average curve for short-circuit current is higher by a factor of five to six over the curve of vacuum emission, as is apparent from Figs. 9 and 10. (The vacuum emission curve has been shown for comparison.) The scatter of the points somewhat obscures the fact that the short-circuit current varies with cesium pressure. When short-circuit current is plotted as a function of cesium pressure (Fig. 11) for an emitter temperature of 2000°K, it is apparent that the current increases with increasing pressure. At cesium temperatures above

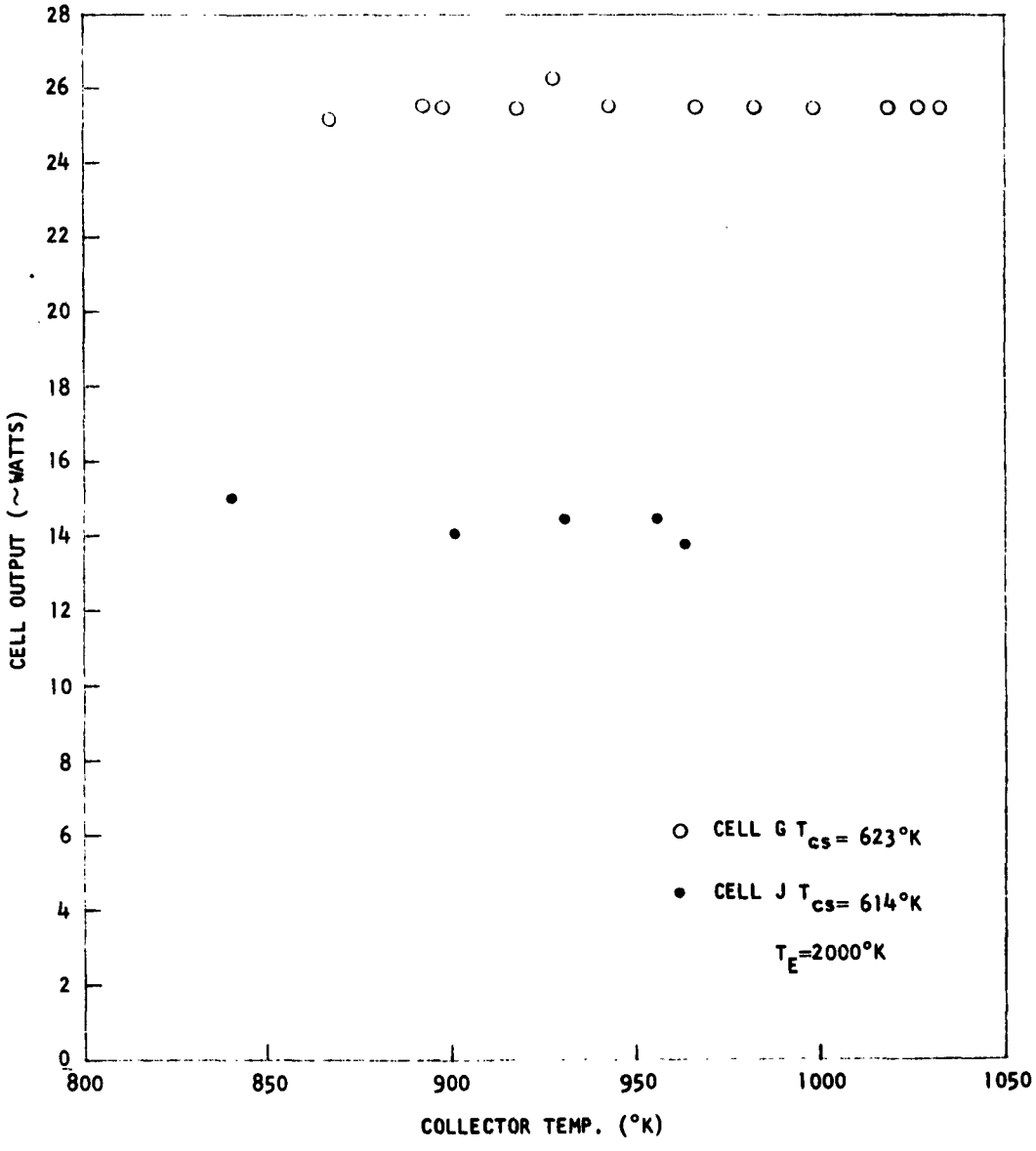

Fig. 8--Effect of collector temperature on power output of Cells G and J

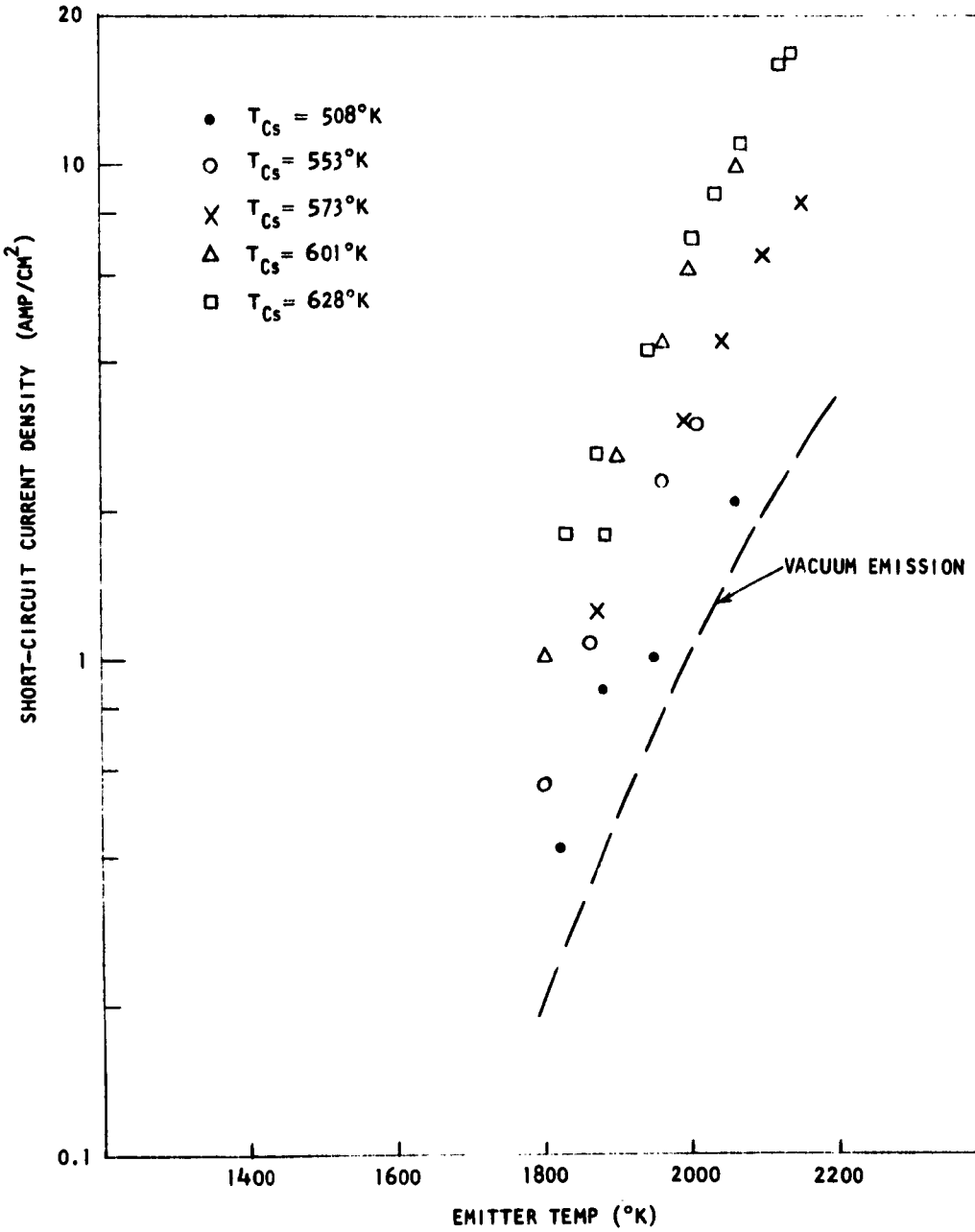

Fig. 9--Short-circuit current density of Cell G as a function of emitter temperature at various cesium temperatures

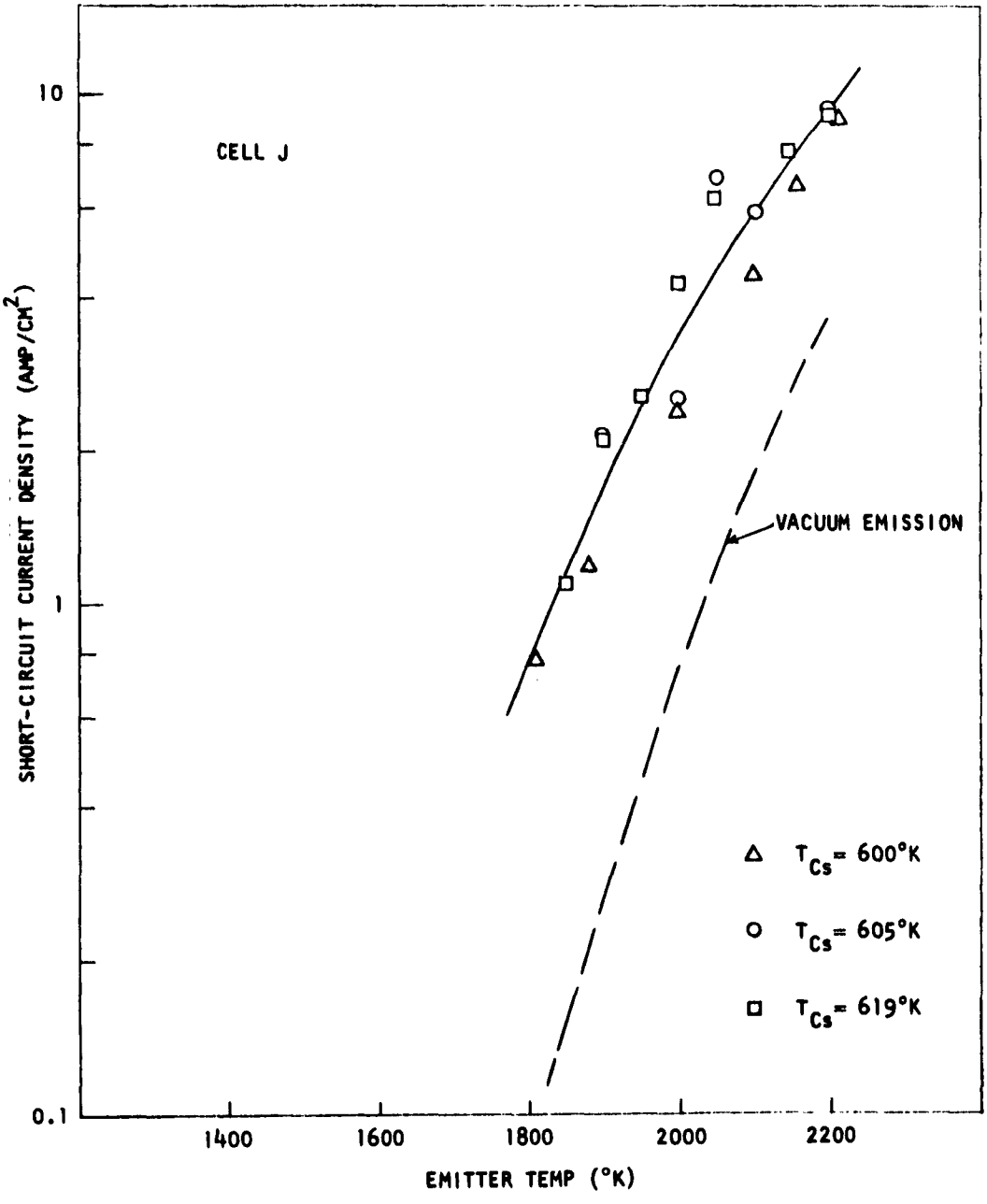

Fig. 10--Short-circuit current density of Cell J as a function of emitter temperature at various cesium temperatures

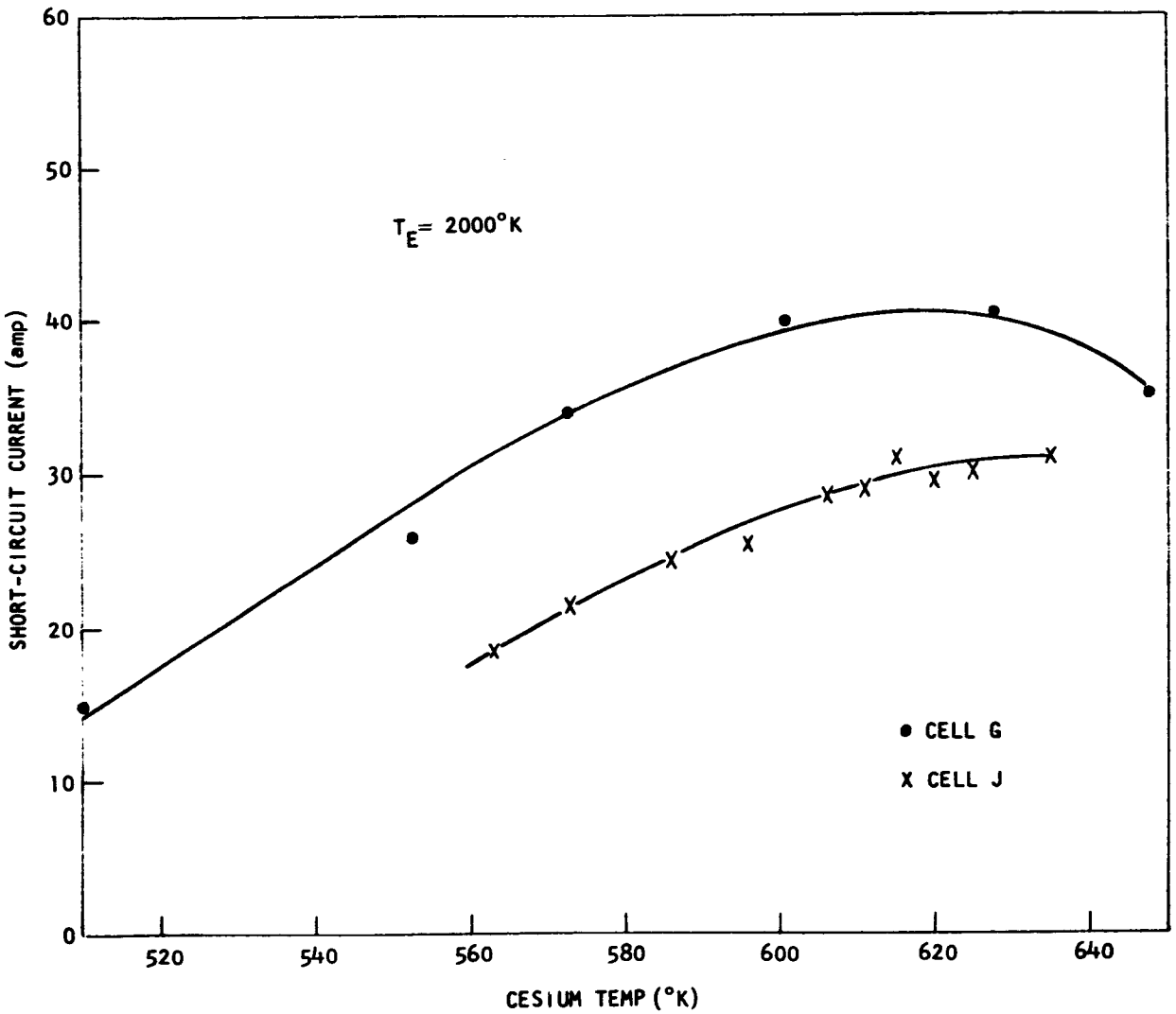

Fig. 11--Short-circuit currents of Cells G and J as a function of emitter temperature

620°K a leveling off occurs, followed by a slight decrease. However, this decrease is not nearly as pronounced as the reduction in power output due to cesium pressures (Fig. 6) above the optimum.

The voltage corresponding to maximum power output is shown in Fig. 12 as a function of cesium pressure. It is of interest that it decreases as a straightline function with increasing cesium temperature from 1.3 volt at 470°K to 0.6 volt at 650°K. It becomes apparent why at cesium pressures above the optimum the power output decreases sharply, since both voltage and current are decreasing.

The open-circuit voltage is likewise a function of the cesium pressure (Fig. 12) and with a slope nearly equal to that of the voltage at maximum power. The open-circuit voltage is dependent upon the emitter temperature and increases from 1.7 volt at 1800°K to 2 volts at 2200°K (Fig. 13). This clearly shows that the work function changes with cesium pressure as well as emitter temperature and that wetting by cesium must occur.

The effective emissivity of the cylindrical carbide emitter in the nickel collector cavity was evaluated. For the purpose of the study, it was assumed that the power input (P_{in}) at open-circuit and steady-state condition was equal to the power lost by radiation from the emitter only. The losses by conduction down the emitter stem and convection through the plasma were considered negligible. Furthermore, it was assumed that all the electrical power input was dissipated in the emitter cavity only (no lead losses). Then the power input is $P_{in} = EAT^4$. For blackbody radiation in which E = 1 and $P_{BB} = AT^4$, P_{BB} can be computed at a given temperature T with an emitter area of 12 cm^2. The effective emissivity E then becomes $E = P_{in}/P_{BB}$.

This emissivity is plotted in Fig. 14 for Cells G and J together with the corresponding collector temperature. The effective emissivity decreased 12% with an emitter temperature increase of 300°K. The average emissivity is 0.55 ± 0.05 at 2000°K.

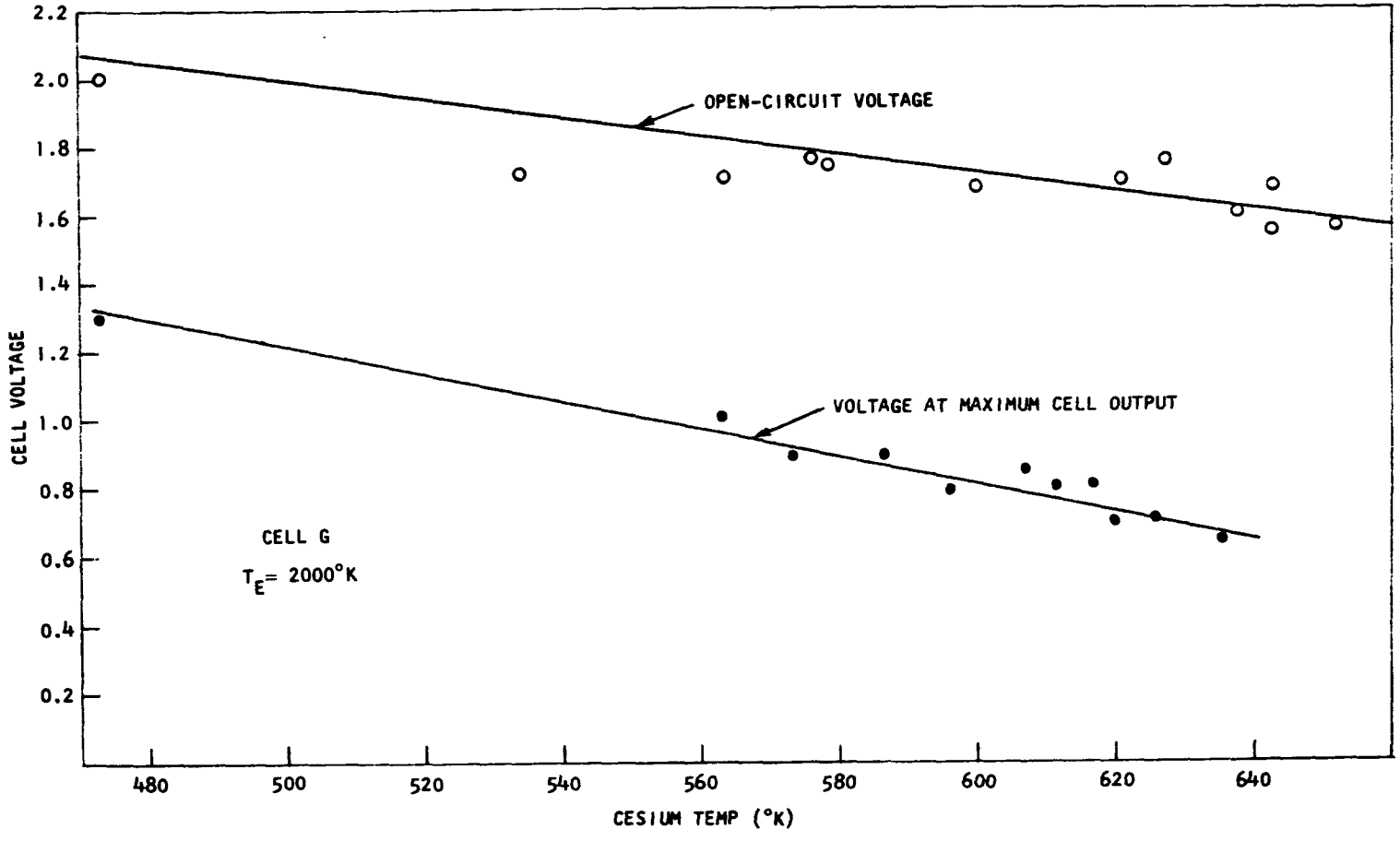

Fig. 12--Variation of cell voltage with cesium temperature

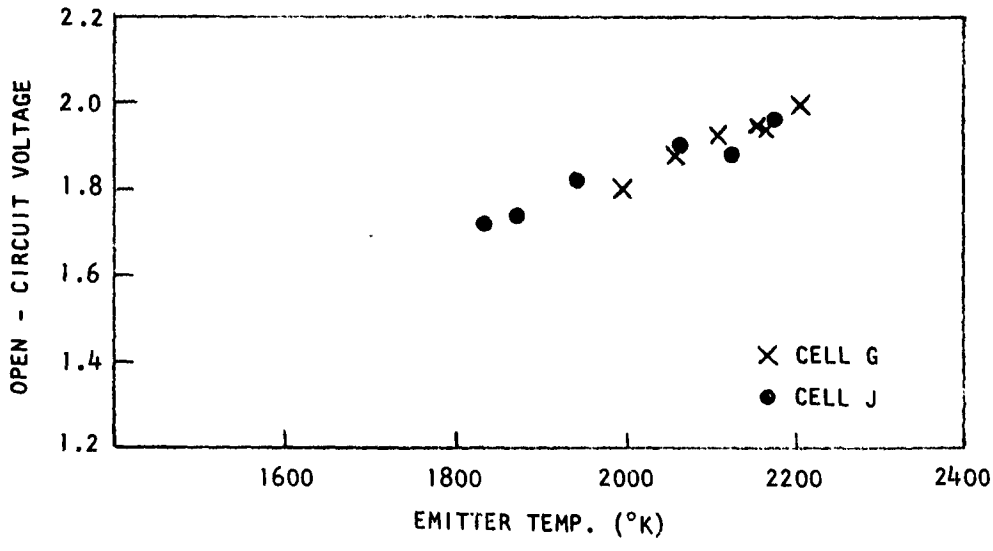

Fig. 13--Variation of open-circuit voltage of Cells G and J with emitter temperature

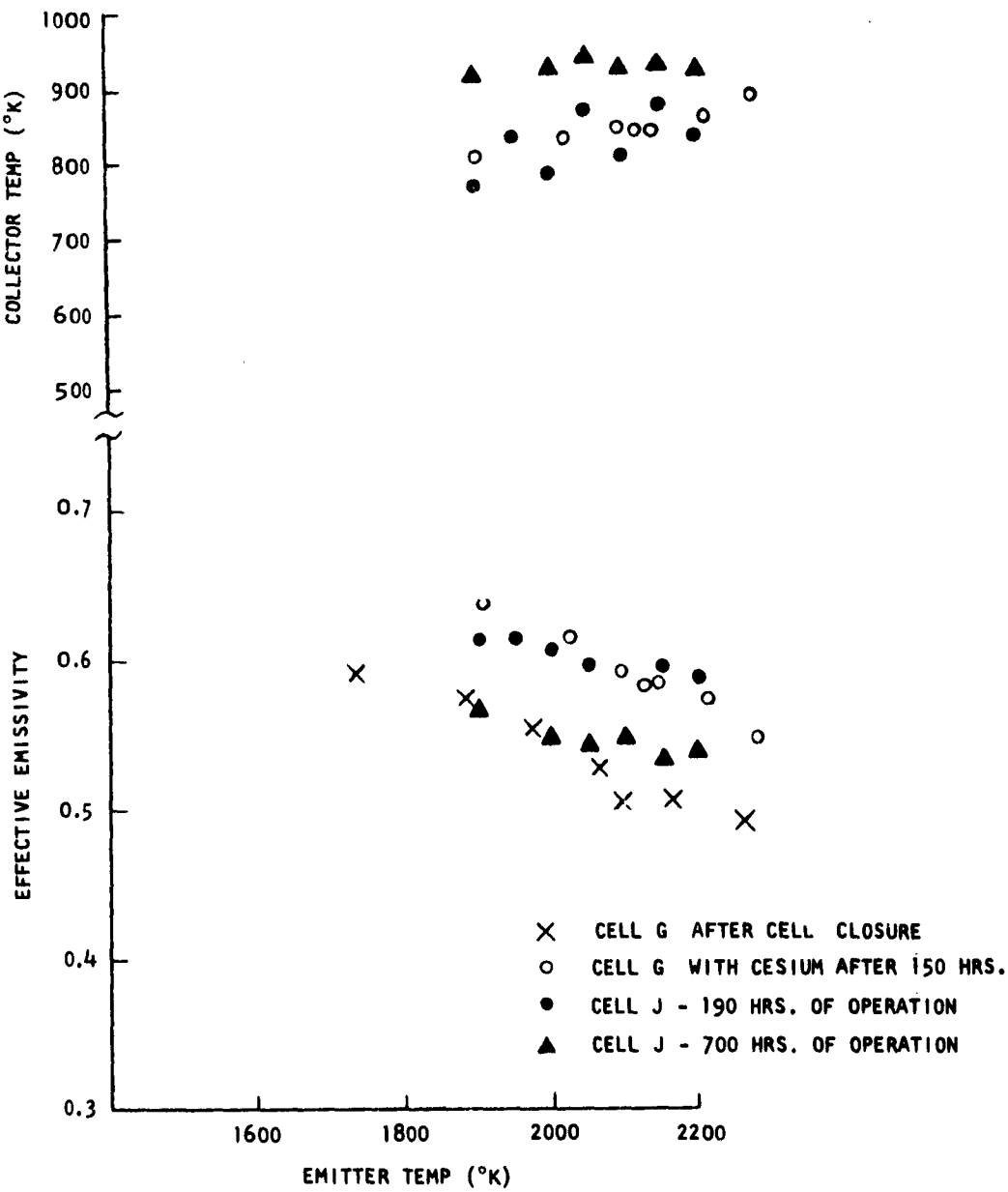

Fig. 14--Variation of emissivity and collector temperature of Cells G and J with emitter temperature

The corresponding collector temperatures are plotted in the same figure to show how they increased with emitter temperature. Since collector cooling was not very effective, increasing emitter temperature resulted in higher collector temperatures. After Cell J had been operated for 700 hr, an emissivity check made at nearly constant collector temperature revealed that the effective emissivity had not changed over 500 hr of operation and that a higher collector temperature resulted in a lower effective emissivity.

Cell G had operated for a total of 1753 hr (Fig. 15) before a large power degradation was observed. During this time the only interruptions were three electron-gun filament failures. Brushes on the collector cooling oil pump wore out several times; however, the cell was not shutdown but rather the collector was allowed to float up in temperature while the brushes were replaced. There was some intermittent collector-to-emitter shorting, particularly during large changes of emitter temperature and corresponding collector temperature changes. After thermal equilibrium had been reached, the shorting problem disappeared. Final cell degradation could be traced to loss of cesium through leaks in welds.

During unattended operation the output of Cell G varied between 12 and 18 watts for 1662 hr. Then the emitter temperature was raised to obtain an output of over 20 watts. During this time, collector cooling oil flow was not on and the collector temperature floated up to 1090°K.

The maximum power output observed on any cell was 68 watts. It was obtained at an emitter temperature of 2120°K, a collector temperature of 953°K, and a cesium temperature of 628°K. The efficiency computed on the basis of total input power versus output was 6%. At a 20-watt output, the efficiency was 2%.

Cell J was operated for 1249 hr at a power level between 12 and 17 watts without any indication of power degradation (Fig. 16). After a period of 24 hr above 30 watts, the emitter temperature was increased to obtain an

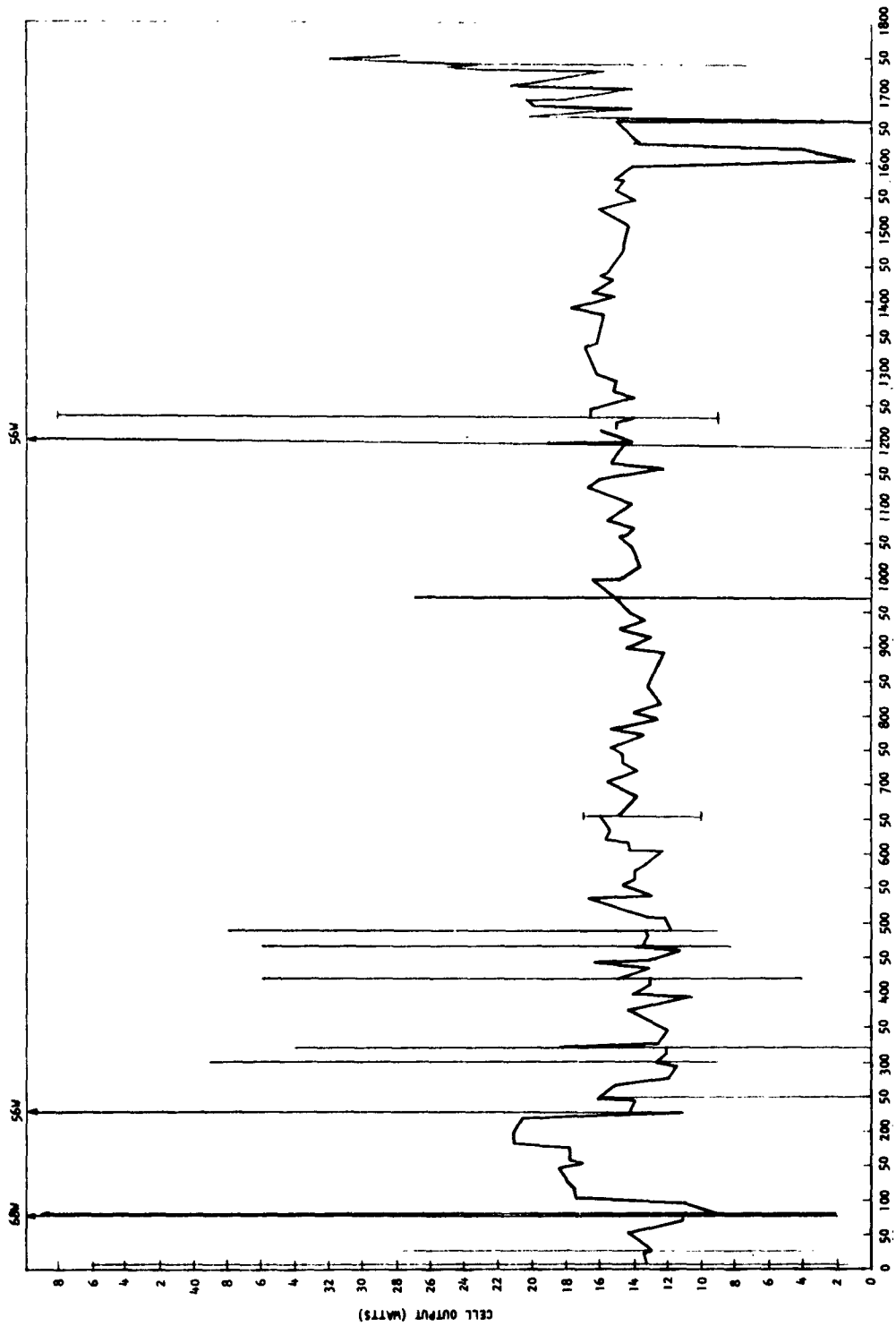

Fig. 15--Power output of Cell G as a function of hours of operation

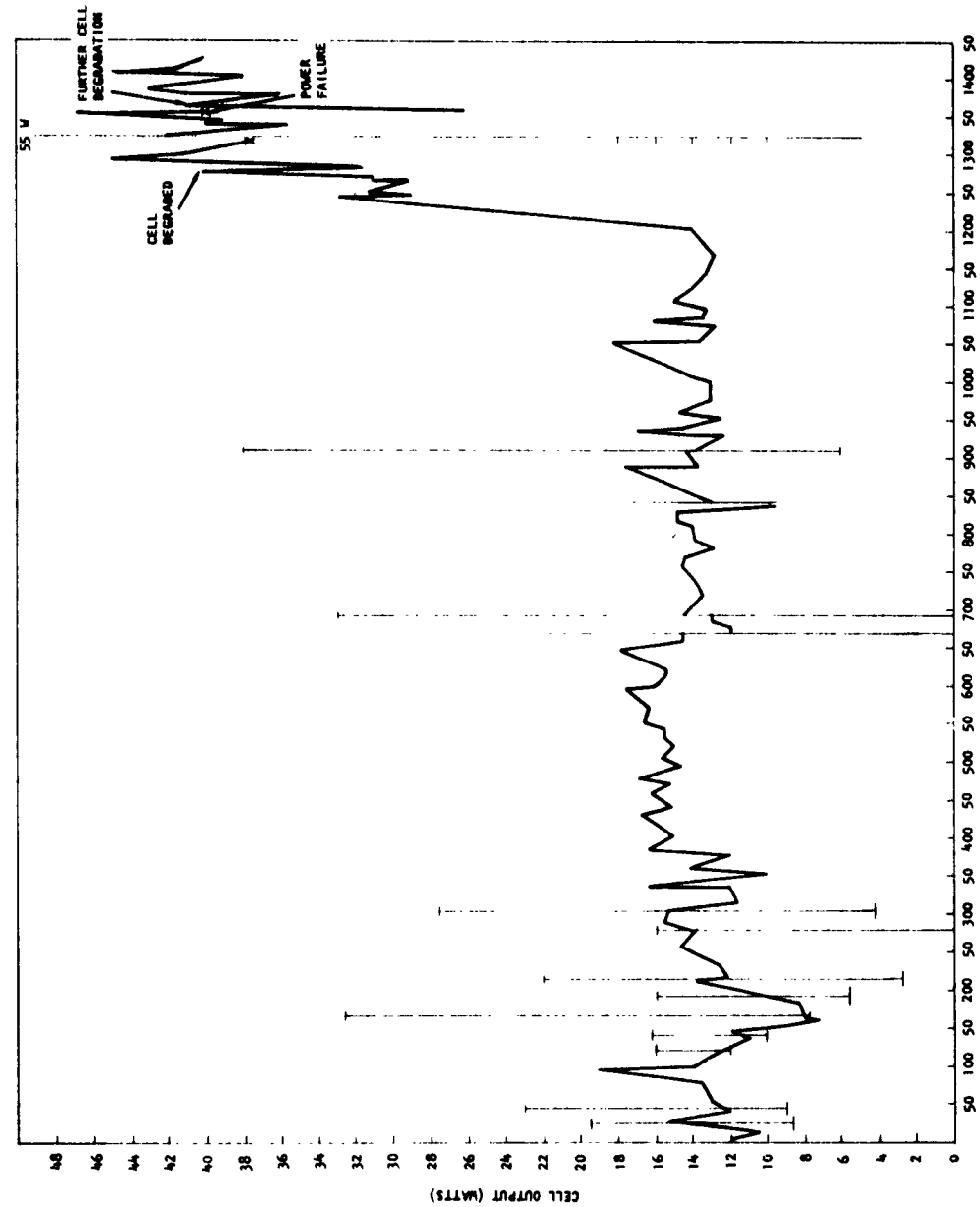

Fig. 16--Power output of Cell J as a function of hours of operation

average output of 40 watts. Also for this cell the collector coolant system was not operated during the final days and the collector temperature varied between 1130 and 1160°K. The cell operated up to 47 watts for 151 hr with an efficiency of up to 37% before the third filament failure occurred. After filament replacement, the power output had degraded by a factor of 10. Again the evidence conclusively pointed to a loss of cesium.

A post-operative analysis will be conducted on Cells G and J to establish what metallurgical and chemical reactions have occurred during the extended hours of operation and thus obtain a better insight into cell operation.

OPERATION OF CELLS IN PARALLEL AND SERIES

During the operation of Cells F, G, and J, the electrical output of two cells was connected either in series or in parallel. These studies were conducted under a variety of load conditions and with independently variable emitter temperatures in the two cells. The data obtained from Cells G and F are presented in Table 1. Because of the very low power output of Cell F, the information was not conclusive.

When Cells J and G were operating simultaneously, network studies were conducted again. The electrical circuitry used for these measurements is shown in Fig. 17. Since the two cells were completely independent of each other, except for the electrical connection, no interaction between the cells was observed. The data obtained are shown in Tables 2 and 3. The results agree with the principle of current conservation within experimental accuracy. Circuit voltage conditions under parallel operation are consistent with lead resistances of 0.011 ± 0.001 ohm in series with each cell. Current and voltage data for series operation are consistent with a circuit resistance of 0.006 ± 0.002 ohm in addition to the variable-load resistance.

Table 1

SERIES AND PARALLEL OPERATION OF CELL F AND CELL G

Cell F and Cell G in Parallel
(for various load resistances)

Cell F		Cell G		Total		Remarks
V (volts)	I (amp)	V (volts)	I (amp)	V (volts)	I (amp)	
0.85	3.2	0.95	7	0.84	9.5	
0.75	3.9	0.89	8	0.73	12.5	
0.62	6	0.75	10	0.58	16.5	
0.9	2.7	1.25	20	0.84	24	Increased emitter temp. of Cell G
0.47	9.9	0.87	22	0.40	34	

Cells F and G in Series

Cell F		Cell G		Total		Remarks
V (volts)	I (amp)	V (volts)	I (amp)	V (volts)	I (amp)	
0.6	8	0.3	8	0.74	8.2	
0.24	15	1.42	14.6	1.34	15	Increased emitter temp. of Cell G

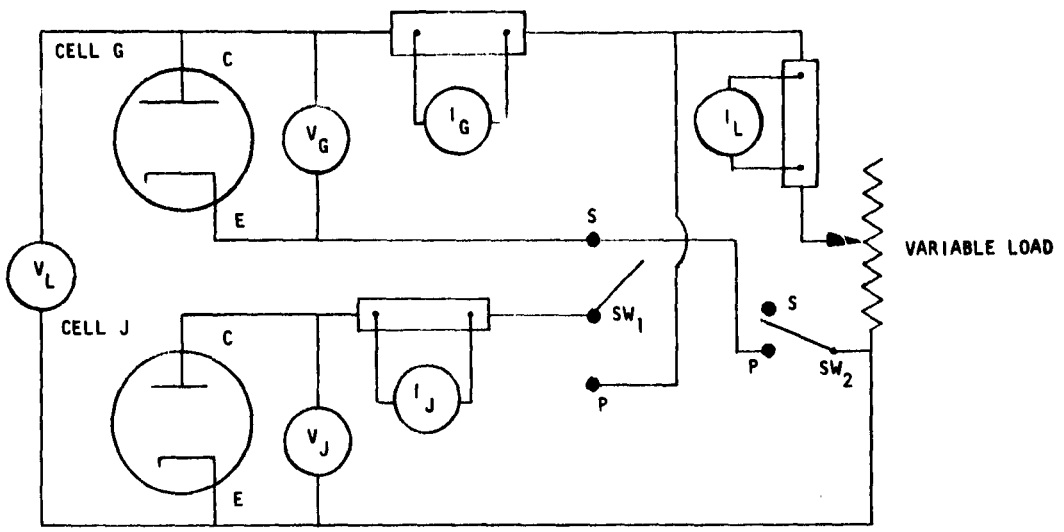

V = VOLTAGE

I = CURRENT

E = EMITTER

C = COLLECTOR

S = SERIES CONNECTION

P = PARALLEL CONNECTION

SW = SWITCH

SUBSCRIPT

G = CELL G

J = CELL J

L = LOAD

Fig. 17--Circuit to measure operation of Cells G and J in series and parallel

Table 2

CELLS CONNECTED IN PARALLEL

Cesium Temperature - 618°K

CELL G			CELL J			LOAD		
Emitter Temp. (°K)	Cell Voltage (V_G)	Cell Current (I_G)	Emitter Temp. (°K)	Cell Voltage (V_J)	Cell Current (I_G)	Voltage (V_L)	Current (I_L)	Power (watts)
2051	0.98	15	2010	0.95	12.5	0.81	27	21.9
2102	1.19	10.5	2022	1.17	9.2	1.08	19	20.5
2080	0.94	16	2005	0.91	13.5	0.76	29	22.1
			Increased Cell G emitter temperature					
2146	1.05	19	2005	0.99	12	0.84	31	26
2120	0.8	25.5	2000	0.73	15.8	0.52	41	21.3
2195	1.33	13	2040	1.28	7.8	1.19	20	23.9
			Increased Cell J emitter temperature					
2182	1.15	17.5	2115	1.14	18.5	0.94	36.5	34.4
2085	0.82	24.5	2082	0.82	24.5	0.54	48.5	26.2

Table 3

CELLS CONNECTED IN SERIES

CELL G			CELL J			LOAD		
Emitter Temp. (^{O}K)	Cell Voltage (V_G)	Cell Current (A_G)	Emitter Temp. (^{O}K)	Cell Voltage (V_J)	Cell Current (A_J)	Voltage (V_L)	Current (A_L)	Power (watts)
2109	0.46	33	2088	0.58	31	0.88	31	27.2
2108	0.55	29	2088	0.67	28.5	1.08	28.5	30.8
2120	0.70	27	2098	0.80	27	1.38	27	37.4
2122	0.73	24	2110	0.97	23	1.57	23.5	37
2150	0.99	21.5	2120	1.10	21	1.95	21.0	41
2155	0.96	18.75	2130	1.18	18.5	2	18	36
			Decreased Cell J Emitter Temperature					
2185	1.14	18	2045	0.94	17.5	1.95	17.5	34
2156	1.0	21	2028	0.71	20.5	1.57	20.5	32.2
			Decreased Cell G Emitter Temperature					
2022	1.6	18.5	2040	0.9	18	1.35	18	26
2025	0.75	16.5	2045	0.99	16	1.63	16	26
2020	0.82	15.8	2050	1.05	15	1.75	15	26.4
2026	0.91	14	2060	1.14	13	1.95	13.5	26.4

FISSION-PRODUCT CONTAMINATION OF THERMIONIC CONVERTERS

In the absence of data on the effect of various fission products on cell performance, an analysis of the fate of the fission products in a thermionic cell environment was performed purely from a chemical standpoint. It was assumed that

(1) Bare UC-ZrC emitters operated at 1900°C

(2) Collectors operated at 900°C

(3) Cesium pressure = 10 mm Hg at a reservoir temperature of 370°C

(4) 15 cm^3 void volume in cell.

The fission-product elements most likely to remain in the cathode are zirconium, molybdenum, technetium, ruthenium, and rhodium. Yttrium and the less volatile rare earth elements (lanthanum, cerium, praseodymium, neodymium, and gadolinium), even though they tend to form stable carbides, will be somewhat volatile at 1900°C, while samarium and europium will be quite volatile. Release of the fission products will be determined by their rate of diffusion from the UC-ZrC matrix in which they are born, as well as by their volatility; but diffusion at 1900°C will probably be too fast to hold down release of fission products over periods of hundreds to thousands of hours.

The noble gas fission products of krypton and xenon will not affect the converter as long as the thermionic converter cells are vented to prevent undue pressure buildup.

The electronegative fission products selenium, bromine, tellurium, and iodine will tend to combine with cesium and thereby have their effects greatly reduced. Of the halogen fission products, iodine is the most important because of its higher fission yield; but it will tend to form cesium iodide (the most stable iodide known from the standpoint of heat of formation per iodine atom) and condense in the cesium reservoir. At a reservoir temperature of 370°C, the vapor pressure of cesium iodide is estimated

to be 2×10^{-8} atm. In the presence of cesium, the vapor pressure of selenium and tellurium will be still lower. The electronegative fission products will also show a tendency to combine with alkaline earth and rare earth fission-product elements and accumulate in the cesium reservoir as salts of these elements.

There is a great excess of electropositive elements formed in fission. As is indicated in Table 4, the yield of cesium itself is high (18% of fission) and that of rubidium is lower (3.5%). The relatively volatile alkaline earth elements strontium and barium are yielded in substantial amounts (9.4 and 5.7%, respectively). The rare earth elements are formed to an even greater extent, the yields of Y, La, Ce, Pr, Nd, Pm and Sm adding up to 54.9%

If a converter cell runs for the order of 10,000 hr and a volatile fission product is not subject to condensation or dissolution in the cesium of the reservoir, enough products are formed to give the order of 1 atm at 900°C per 1% of fission yield. Thus, ample quantities of the elements would be formed to lead to condensation on the anode (at 900°C) if it were not for the lower temperature of the cesium reservoir. Actually, about half of the fission products, comprising the more volatile electropositive and the electronegative elements (the order of 20 millimoles in 10,000 hr in a cell with 15 cm^3 of free volume), will tend to condense in the cesium reservoir. However, they will also tend, to an undetermined degree, to contaminate (sorb on) the anode and to be present in the vapor or plasma phase.

Table 4

PERCENTAGE YIELD OF VARIOUS ELEMENTS
AS FISSION PRODUCTS

Element	Fission Yield of Element ΣY (%)	b.p. ($^{\circ}$K) of Element
Ge	0.00232	3,100
As	0.0008	866
Se	0.485	958
Br	0.14	331.4
Kr	3.86	119.75
Rb	3.5	974
Sr	9.4	1,640
Y	4.8	(3,500)
Zr	31.0	4,650
Nb	0	5,200
Mo	24.5	5,100
Tc	6.1	4,900
Ru	11.3	(4,000)
Rh	3.0	(4,000)
Pd	1.17	3,400
Ag	0.03	2,450
Cd	0.097	1,038
In	0.011	2,320
Sn	0.095	2,960
Sb	0.058	1,910
Te	2.42	1,260
I	1.03	456
Xe	22.3	165.04
Cs	18.0	958
Ba	5.7	1,910
La	6.2	3,640
Ce	12.4	3,200
Pr	6.0	3,290
Nd	21.2	3,360
Pm	2.4	(3,000)
Sm	1.92	(1,860)
Eu	0.183	(1,700)
Gd	0.015	(3,000)
Tb	0.0011	(2,800)
Dy	0.00005	2,600

REFERENCES

1. Godsin, W., High-Temperature Vapor-Filled Thermionic Converter, Quarterly Technical Progress Report for the Period October 1 through December 31, 1962, General Atomic Report GA-3798, January 7, 1963.

2. Godsin, W., High-Temperature Vapor-Filled Thermionic Converter, Quarterly Technical Progress Report for the Period July 1 through September 30, 1962, General Atomic Report GA-3562 (Rev.), November 10, 1962.